QCD AT ATLAS: THE STORY SO FAR

Paul NEWMAN (on behalf of the ATLAS Collaboration)

School of Physics & Astronomy, University of Birmingham, B15 2TT, UK

Many of the earliest ATLAS results based on 2010 LHC data are focused on strong interaction dynamics. This contribution reports on a selection of these results, including minimum bias observables, hard scattering cross sections and the first heavy ion collision data.

1. Introduction

Since the start of Large Hadron Collider (LHC) operation at $\sqrt{s} = 7$ TeV in Spring 2010, the number of collisions produced has grown roughly exponentially with running time. By the end of the 2010 run, a sample of integrated luminosity around 45 pb^{-1} had been collected, at a peak luminosity of around 10^{32} cm^{-2}s^{-1}. In addition, the first LHC run with lead ion collisions in November yielded approximately 9 μb^{-1} at a nucleon-nucleon centre of mass energy of $\sqrt{s} = 2.76$ TeV. The ATLAS detector [1] performed well throughout the 2010 run and its response was quickly understood. The results contained in this talk [2] are based on varying sample sizes taken from the 2010 data. LHC physics is an extremely fast-moving field. By the time of writing (May 2011), the 2011 data sample has already reached an integrated luminosity of over 250 pb^{-1}, such that many of the results here will soon be superceded. For a complete current list of ATLAS publications and preliminary results, see [3].

2. Minimum Bias Data

At low luminosities, ATLAS operated a trigger using the Minimum Bias Trigger Scintillators (MBTS), which cover the pseudorapidity range $2.1 < |\eta| < 3.8$ with high efficiency to detect charged particles. Samples collected with this trigger are thus close to an unbiased mixture of all inelastic pp processes. The exception is a lack of acceptance for diffractive dissociation processes $pp \to pX$ and $pp \to XY$, where the masses of the systems X and Y are sufficiently small that no particles are produced with

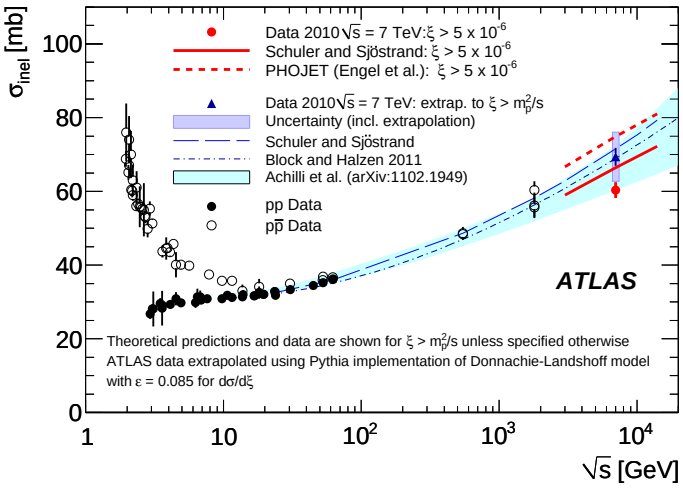

Fig. 1. Measurements of the total inelastic pp and $\bar{p}p$ cross sections as a function of centre of mass energy, compared with a variety of models. The ATLAS measurement [4] is also shown and compared with the predictions of the PYTHIA and PHOJET MC models before extrapolation to the unmeasured region $\xi < 5 \times 10^{-6}$.

$|\eta| < 3.8$. An MBTS-triggered sample has therefore been used to measure the inelastic cross section in the kinematic range $\xi = M_X^2/s > 5 \times 10^{-6}$, M_X being the larger mass of the two final state systems and s being the square of the centre of mass energy. The result is shown in figure 1 [4]. The uncertainty of 3.5% is heavily dominated by the luminosity measurement. The resulting cross section lies below the predictions of the standard Monte Carlo (MC) models of minimum bias physics, PYTHIA [5] and PHOJET [6], the latter exhibiting the more significant discrepancy. Extrapolating this result to the total inelastic pp cross section via a factor of 1.11 ± 0.10 allows comparison with a wider range of models, based on Regge phenomenology [5], a logarithmic cross section growth [7] or a QCD-based approach [8]. Models in all of these categories are able to describe the data.

The characteristics of minimum bias pp events are investigated through the study of the charged particles reconstructed in the Inner Detector. The resulting data provide a precise and powerful tool for the optimisation and tuning of minimum bias MC models. An example inclusive charged particle measurement [9] is shown in figure 2a. The event-normalised distribution in the total number of charged particles with transverse momentum $p_T > 100$ MeV produced within the tracking acceptance $|\eta| < 2.5$ is shown. Contributions with up to 200 charged particles are observed, none of the MC models giving a complete description of the distribution.

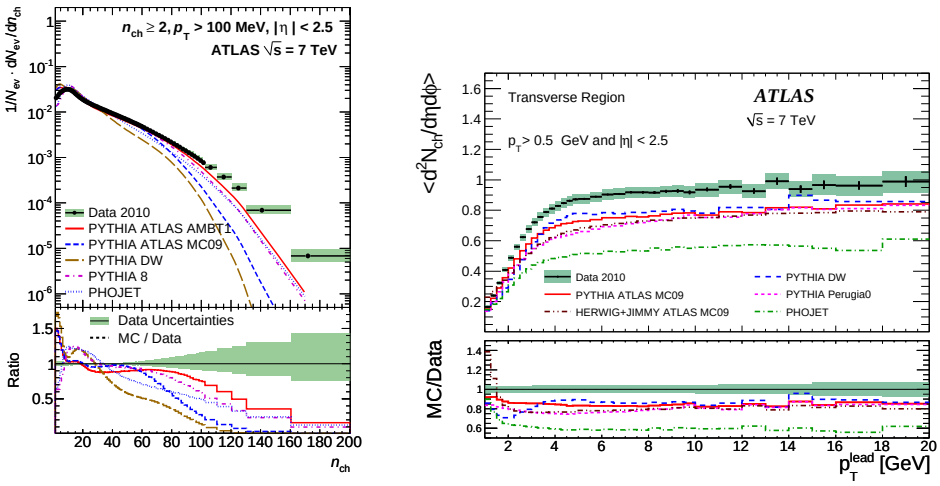

Fig. 2. (a) Inclusive central charged particle multiplicity distribution [9]. (b) Central charged particle multiplicities as a function of transverse momentum restricted to azimuthal angles transverse to the leading particle [10]. In both cases, minimum bias pp data are compared with Monte Carlo models.

The charged particle samples have also been used to investigate the underlying event [10], which accompanies all hard proton-proton collisions due to multiple parton interactions and beam remnant effects. The charged particles in every event are categorised according to their azimuthal angles ϕ. A 'toward' region is then defined by the ϕ value of the highest p_T track, which strongly correlates with the ϕ of the hardest scattering in the event. A 'transverse' region is then defined by $60^o < |\Delta\phi| < 120^o$, with $\Delta\phi$ measured relative to the leading track. Little activity associated with the hard scatter is expected in this region and it is thus the most sensitive to underlying event effects. Figure 2b shows the average number of central charged particles ($|\eta| < 2.5$, $p_T > 500$ MeV) per event in the transverse $\Delta\phi$ region. The level of activity is larger than that predicted by the underlying event model in PYTHIA (MC09 tune [11]) or by HERWIG [12] interfaced to the JIMMY [13] multiple interactions model. An underlying event analysis has also now been performed using calorimeter information with similar conclusions [14].

3. QCD Hard Scattering

The ATLAS data taken in 2010 are already more than adequate for the study of a variety of hard processes initiated by the quarks and gluons from the colliding protons. The resulting data are being used to test perturbative QCD and our knowledge of the proton parton densities. First measurements

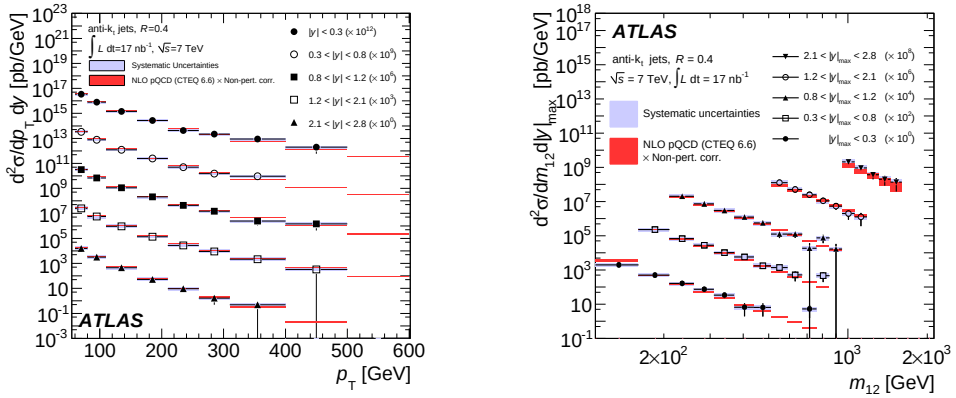

Fig. 3. (a) Double differential cross section in jet rapidity and transverse momentum for inclusive jets. (b) Double differential cross section in rapidity and dijet invariant mass for dijets. In both cases, pp scattering data [17] are compared with an NLO QCD prediction.

of W and Z production cross sections, which are dominated by $q\bar{q}$ fusion, are published in [15] and agree well with predictions, as do measurements of electroweak gauge bosons in association with jets [16].

In contrast to electroweak gauge boson production, hadronic jet data are primarily sensitive to the proton gluon density via the processes $gg \to gg$ and $gg \to q\bar{q}$. The first ATLAS inclusive jet and dijet data were published using a data sample with an integrated luminosity of a mere 17 nb^{-1} [17], by which time, the jet energy scale was already known to 6% and the sample size was sufficiently large to make measurements over a wider kinematic range than has been explored hitherto. An example p_T distribution for inclusive jets, also differential in jet rapidity y, is shown in figure 3a. Good agreement is observed with a next-to-leading order (NLO) QCD calculation [18] using the CTEQ6.6 parton densities [19], the distribution extending to $p_T = 600$ GeV. A double differential dijet cross section as a function of y and the dijet invariant mass is shown in figure 3b. Good agreement with NLO QCD is again observed, with dijet invariant masses of almost 2 TeV being produced. On the basis of these data, world-leading limits have been set on quark compositeness and related models for new physics [20].

Further analysis of dijet data has been focused on variables which are sensitive to the pattern of QCD radiation. Jet shape measurements [21] quantify the transverse momentum density as a function of distance from the jet seed direction in $\eta - \phi$ space. Azimuthal decorrelation measurements [22] assess the difference in ϕ between the leading and next-to-leading jets in an event. In both cases, ATLAS data show reasonable agreement with

appropriately tuned model predictions.

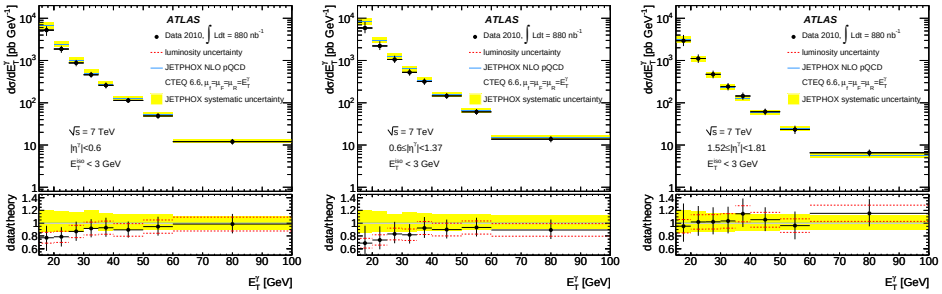

Fig. 4. Isolated photon cross sections [23] as a function of photon transverse energy in three rapidity regions. pp scattering data are compared with NLO predictions.

A final category of hard scattering process, direct photon production, is driven doninantly by the subprocess $qg \to q\gamma$ at LHC energies. Meausurements of isolated high p_T photon cross sections are shown in three rapidity ranges in figure 4 [23]. Once again there is good agreement with NLO QCD predictions [24], except in the central rapidity region, where there is evidence for discrepancies at the smallest p_T values. This may be attributed to deficiencies in the theoretical treatment of fragmentation contributions or scale choices.

4. Heavy Ion Collisions

The lead-lead data at $\sqrt{s}_{NN} = 2.76$ TeV were taken at a centre of mass energy more than 10 times larger than that of previous measurements at RHIC. ATLAS offers near-hermetic detector acceptance for the comprehensive study of these collisions. The data were triggered using the MBTS and are classified in terms of a 'centrality' variable, which is derived from forward energy flow measurements and is closely correlated with the impact parameter between the two incoming ions, equivalently the number of primary nucleon-nucleon binary collisions. The data contain a promising sample of Z bosons, and a large sample of J/ψ mesons [25]. The latter have been used to confirm the observation of J/ψ suppression relative to appropriately scaled pp yields, becoming more significant for increasingly central collisions, as previously observed at the SPS [26] and RHIC [27]. This result is consistent with the expected phenomenon of colour screening in dense nuclear matter [28].

The first direct observation of the jet quenching phenomenon [29] has been made by ATLAS [30], following the reports of closely related effects for high transverse momentum single particle production at RHIC [31, 32].

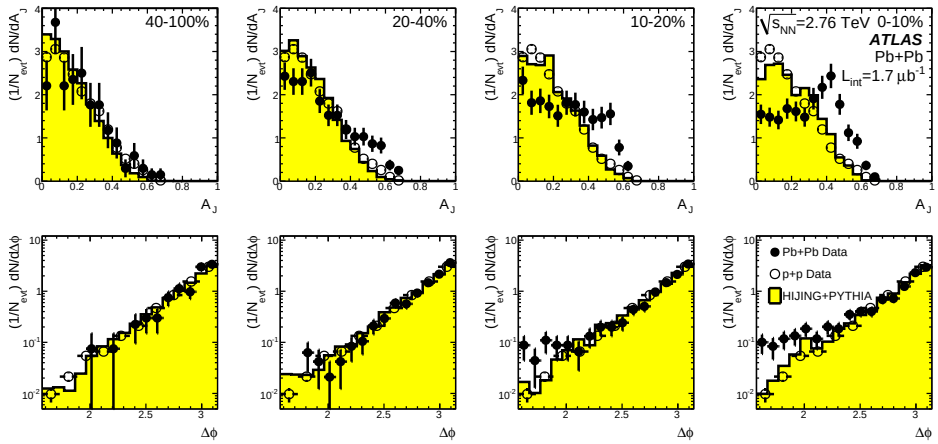

Fig. 5. Top row: asymmetry between the transverse energies of the two leading jets in heavy ion collisions. Bottom row: azimuthal decorrelation between the two leading jets. In both cases, the data are divided according to centrality, with the most peripheral collisions on the left and the most central collisions on the right [30].

Here, an imballance between leading and next-to-leading jet energies is observed for the most central collisions, suggesting that the transverse momentum is dissipated as partons move through hot dense nuclear matter, in a manner which is consistent with quark-gluon plasma formation. Figure 5 (top) shows centrality-dependent measurements of the asymmetry $A_J = (E_{T1} - E_{T2})/(E_{T1} + E_{T2})$ between the transverse energies E_{T1} and E_{T2} of the leading and next-to-leading jets, respectively, after application of the cuts $E_{T1} > 100$ GeV and $E_{T2} > 25$ GeV. In peripheral collisions, where the outgoing partons pass through minimal nuclear matter, the measured distribution is compatible with that for pp data at $\sqrt{s} = 7$ TeV and is well described by a MC model which contains no in-medium effects. In contrast, for the most central 10% of collsions, a clear difference is observed between the lead-lead data and the other distributions. As can be inferred from the consistency between the heavy ion data, the MC model and the pp data for the azimuthal decorrelation between the two jets in Figure 5 (bottom), this is not likely to be caused by higher order radiation. The data therefore provide good evidence for parton energy loss in the nuclear medium.

REFERENCES

[1] G. Aad *et al.* [ATLAS Collaboration], JINST **3** (2008) S08003.

[2] Slides: `http://cdsweb.cern.ch/record/1356583/files/ATL-PHYS-SLIDE-2011-238.pdf`.

[3] `https://twiki.cern.ch/twiki/bin/view/AtlasPublic`.

[4] G. Aad *et al.* [ATLAS Collaboration], *"Measurement of the Inelastic Proton-Proton Cross-Section at $\sqrt{s} = 7$ TeV with the ATLAS Detector,"* arXiv:1104.0326 [hep-ex], submitted to Nature Communications.

[5] T. Sjostrand, S. Mrenna and P. Skands, Comput. Phys. Commun. **178** (2008) 852; idem JHEP **0605** (2006) 026.

[6] R. Engel, Z. Phys. C **66** (1995) 203.

[7] M. Block and F. Halzen, Phys. Rev. D **83** (2011) 077901.

[8] A. Achilli et al., arXiv:1102.1949 [hep-ph].

[9] G. Aad *et al.* [ATLAS Collaboration], arXiv:1012.5104 [hep-ex] (accepted by New J. Phys.).

[10] G. Aad *et al.* [ATLAS Collaboration], arXiv:1012.0791 [hep-ex] (accepred by Phys. Rev. D.).

[11] G. Aad et al. [ATLAS Collaboration], ATLAS Monte Carlo tunes for MC09, (2010), ATL-PHYS-PUB-2010-002.

[12] G. Corcella *et al.*, arXiv:hep-ph/0210213.

[13] J. Butterworth, J. Forshaw and M. Seymour, Z. Phys. C **72** (1996) 637.

[14] G. Aad *et al.* [ATLAS Collaboration], Eur. Phys. J. C **71** (2011) 1636.

[15] G. Aad *et al.* [ATLAS Collaboration], JHEP **1012** (2010) 060.

[16] G. Aad *et al.* [ATLAS Collaboration], Phys. Lett. B **698** (2011) 325.

[17] G. Aad *et al.* [ATLAS Collaboration], Eur. Phys. J. C **71** (2011) 1512.

[18] Z. Nagy, Phys. Rev. D **68** (2003) 094002.

[19] P. Nadolsky *et al.*, Phys. Rev. D **78** (2008) 013004.

[20] G. Aad *et al.* [ATLAS Collaboration], Phys. Lett. B **694** (2011) 327.

[21] G. Aad *et al.* [ATLAS Collaboration], Phys. Rev. D **83** (2011) 052003.

[22] G. Aad *et al.* [ATLAS Collaboration], Phys. Rev. Lett. **106** (2011) 172002.

[23] G. Aad *et al.* [ATLAS Collaboration], Phys. Rev. D **83** (2011) 052005.

[24] S. Catani, M. Fontannaz, J. Guillet and E. Pilon, JHEP **0205** (2002) 028.

[25] G. Aad *et al.* [ATLAS Collaboration], Phys. Lett. B **697** (2011) 294.

[26] B. Alessandro *et al.* [NA50 Collaboration], Eur. Phys. J. C **39** (2005) 335.

[27] A. Adare *et al.* [PHENIX Collaboration], Phys. Rev. Lett. **98** (2007) 232301.

[28] T. Matsui and H. Satz, Phys. Lett. B **178** (1986) 416.

[29] J. Bjorken FERMILAB-PUB-82-059-THY (1982).

[30] G. Aad *et al.* [ATLAS Collaboration], Phys. Rev. Lett. **105** (2010) 252303.

[31] K. Adcox *et al.* [PHENIX Collaboration], Phys. Rev. Lett. **88** (2002) 022301.

[32] C. Adler *et al.* [STAR Collaboration], Phys. Rev. Lett. **89** (2002) 202301.